

Research Article

CASE STUDIES OF BLACK CARBON AEROSOL CHARACTERISTICS DURING AGRICULTURE CROP RESIDUE BURNING PERIOD OVER PATIALA, PUNJAB, INDIA USING THE SYNERGY OF GROUND BASED AND SATELLITE OBSERVATIONS

Deepti Sharma¹, *Darshan Singh¹ and Sumit Kumar²

¹*Department of Physics, Punjabi University, Patiala (147002), Punjab, India*

²*Michigan Technical University, Houghton, MI, USA*

**Author for correspondence*

ABSTRACT

In the present study, we have examined the variation of BC mass concentration and aerosol properties over Patiala (30.33°N, 76.4°E, 249 m a.s.l) during post-monsoon (PoM) season of the year 2008 using ground based measurements as well as satellite data. Five intense biomass burning cases (13th, 27th, 29th October, 2008 and 07th, 12th November, 2008) have been identified over the study area using Aqua-MODIS true color composites during the study period. BC aerosol mass concentration observed to be high (7-18 $\mu\text{g}/\text{m}^3$) on these days due to crop residue burning over the region. The average values of Aqua-MODIS AOD₅₅₀ and MICROTOPS-II AOD₅₀₀ were 0.98 \pm 0.33 and 1.30 \pm 0.19 respectively while the Aura-OMI derived UV-AI has maximum value of 2.74 during these days. The Angstrom Exponent $\alpha_{380-870}$ and turbidity parameter β varies from 0.89 to 1.41 and 0.40 to 0.68 respectively while aerosol mass concentration (RSPM) reaches to maximum value of 312.6 $\mu\text{g}/\text{m}^3$ during the study period. The negative values of coefficient α_2 indicate the presence of abundance of fine mode particles during PoM-2008. High BC aerosol mass concentration during the days under study results in low Single Scattering Albedo (SSA) varying from 0.70-0.78 due to its absorbing nature. Increased BC concentration during intense biomass burning days leads to high radiative forcing at surface (SRF) and at top of atmosphere (TOA) varying from -67.1 to -95.0 W m⁻² and -3.1 to +3.7 W m⁻², respectively. This results in high atmospheric radiative forcing (ARF) of +92.7 W m⁻² that may result in warming of the lower atmosphere and potentially perturbing the regional climate.

Key Words: *Black Carbon (BC), Radiative Forcing, Aerosol Optical Depth (AOD), Indo Gangetic Plane (IGP)*

INTRODUCTION

Atmospheric aerosols perturb the global climate both directly and indirectly and give rise to radiative forcing (Charlson *et al.*, 1992). Sulfate particles and other non-absorbing aerosols backscatter the solar radiation causing atmospheric and surface cooling. Soot particles such as black carbon (BC) absorb the incoming solar radiation leading to heating of the atmosphere and contributing to the global warming (Charlson *et al.*, 1992; Boucher and Haywood, 2001 and Jacobson, 2001). Beside the direct interactions of aerosols with solar radiation, aerosols cause indirect cooling by modifying the cloud albedo and its rainfall potential. It is still uncertain whether aerosols have net cooling or warming effect on earth's atmosphere because of inadequate quantitative knowledge of regional and global aerosol characteristics and their temporal variations. Biomass burning is one of the significant global sources of atmospheric aerosols and trace gases that have significant impact on the radiative balance of the atmosphere and human health (Kharol and Badrinath, 2006). The major part of these constitutes a carbonaceous aerosol called black carbon (BC), a pollutant of great interest because of its large optical absorption cross-section leading to the warming of the atmosphere. Carbonaceous aerosols under certain conditions may act as condensation nuclei that may change the size distribution, optical properties and rainfall potential of the clouds.

Research Article

In the Indian sub-continent, Indo-Gangetic Planes (IGP) comprising northern India is highly loaded with natural and anthropogenic aerosols with significant temporal and spatial variability in composition and concentration (Gautama *et al.*, 2011). North-west region of India comprising Punjab, Haryana and Uttar Pradesh has experienced increasing levels of farm mechanization over the last two decades. Cultivation and harvesting is now commonly undertaken with farm machinery. Agriculture intensification in this region is inevitable due to increasing population and decreasing per capita agriculture land area. Wheat-rice cultivation is dominant crop rotation and harvesting of these crops with combine harvesters is popular with farmers of Punjab, Haryana and western UP. Tentative estimates show that in Punjab 75-80% under rice is machine harvested leaving behind enormous quantity of residue in the fields (Badrinath *et al.*, 2006). Most of the farmers opt for burning of rice straw as it is a quick and easy approach for disposal of the residue and enable them to prepare the fields for sowing the next wheat crop well in time. This large scale burning of paddy residue in the open fields emit trace gases as well as sub-micron particles such as black carbon (BC) and other organic aerosols resulting in thick cloud of smog enveloping over Punjab and Haryana (Badrinath *et al.*, 2006 and Mittal *et al.*, 2009).

Events with high aerosol optical depth (AOD) with $\tau_\lambda > 1.0$ resulting from biomass burning are common during October-November of every year over Punjab (Sharma *et al.*, 2010). Study of high τ_a smoke cases are of interest as growth mechanisms for aging sub-micron smoke (BC) particles are in part dependent on the concentration of ambient aerosols (Ried *et al.*, 1998). Therefore fine mode particle concentration should reach a maximum during the period of intense biomass burning, given enough time for aging processes to act and may affect the radiative balance of the atmosphere. In the present study, we present the analysis of aerosol optical properties during paddy residue burning period of October–November, 2008 at Patiala; Punjab state (India). More detailed analysis of aerosol properties correspond to five episodes of very high τ_λ due to intense biomass burning and estimated their impact on the atmospheric radiative forcing over the region. We conducted measurements of BC using a 7-channel Aethalometer providing continuous real time data. AOD measurements are made with 5-channel hand held Microtops-II sunphotometer, supplemented with MODIS and OMI satellite data.

Site Description and Meteorology

Patiala (30.2° N, 76.2° E, 249 m a.s.l); is situated in the west part of Indo-Gangetic plain, close to Shivalik Hills in the east and Thar Desert about 300 Km away in the southwest. The observational site is at the roof top of Physics department in the Punjabi university campus, 6 Km away in the north-eastside of the main city. There is no major industry and other anthropogenic sources in the near vicinity of the site and agriculture fields are more than 2 Km away in the north-west and north-east side. University campus has chain of buildings including residential houses and interlinked roads with trees planted on both sides and scattered grassy lawns in the whole campus including a botanical garden. A national high way passes at a distance of about 500m from the south-east side of the observational site.

The climate of the study region is divided in to four seasons viz. winter (December-March), pre-monsoon (April-June), monsoon (July-September) and post-monsoon (October-November). Extreme weather conditions prevail over Punjab as temperature may reach to a minimum value of 0°C during winter and to its maximum value of 45°C during pre-monsoon on certain occasions. Severe fog, haze and smog occur during winter and westerly or north-westerly winds prevail throughout this season. Dust storms are frequent during pre-monsoon due to south-westerly winds that carry the coarse dust particles from the Thar Desert (Sikka, 1997). The climate of the region is also affected by the western disturbances, a well-known synoptic meteorological phenomenon that is prevalent during winter and pre-monsoon seasons. Total rainfall of ~750 mm occurs over Punjab mostly during the monsoon season. During post-monsoon season, mostly dry weather conditions prevail and vast clouds of smoke engulfs the Punjab state due to biomass burning resulting in dim sun shining.

The meteorological parameters were collected from India Meteorological Department observatory situated near the observational site in the university campus. Figure 1 (a, b) shows the daily day time averaged trend of air temperature and relative humidity (RH) during PoM-2008 over Patiala. The daily

Research Article

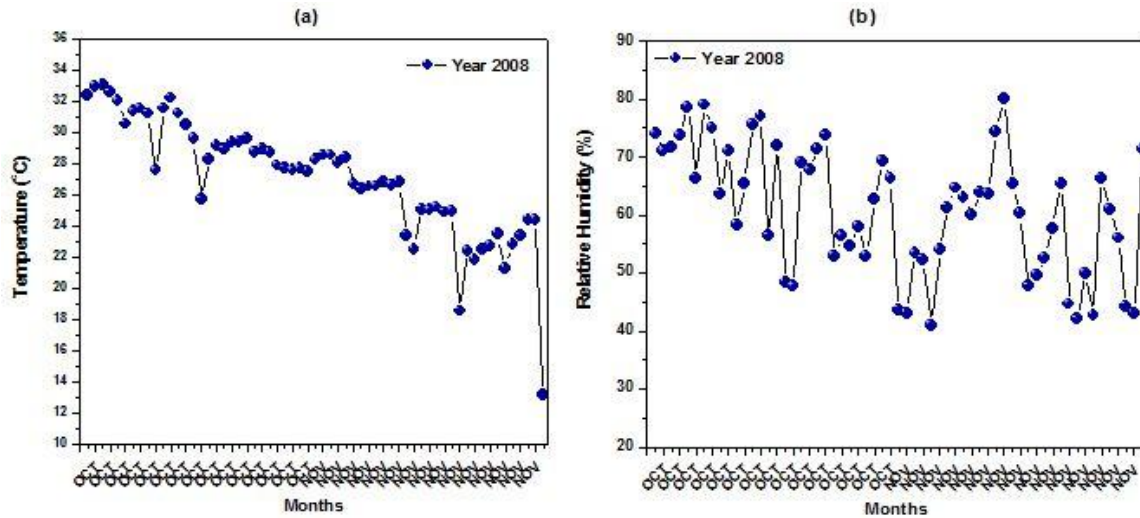


Figure 1: Day to day variation of meteorological parameters (a) temperature (°C) and (b) relative humidity, R_H (%) Patiala during PoM-2008

averaged temperature varies between 26°C to 33°C during October and 13°C to 29°C during November months of 2008. Relative humidity ranged between 43.6%-79% and 41%-80% during October and November, 2008 respectively.

MATERIALS AND METHODS

Aerosol Optical Depth

Aerosol optical depth (AOD) measurements are made using a handheld multichannel MICROTOPS II sun photometer of Solar Light Company, USA (Porter *et al.*, 2001 and Morys *et al.*, 2001). Simultaneously, it measures AOD at five wavelengths viz. 380, 440, 500, 675, 870 nm with each filter having narrow bandwidth of around 10 nm. The spectral variation of AOD can be characterized using Ångström relation (Ångström, 1964).

$$\tau_\lambda = \beta \lambda^{-\alpha} \quad (1)$$

Where τ_λ the AOD at wavelength λ , “ β ” is known as turbidity parameter and “ α ” is the Ångström exponent that depends on the size distribution of aerosols. The Ångström formula can be related to Junge’s power law (Junge, 1955) as;

$$\frac{dN}{d(\ln r)} = cr^{-v} \quad (2)$$

Where dN is the number concentration of the particles with radii between r and $r+dr$ and c and v are fitting parameters. Mie theory states that for spherical particles in the range $0.1 < r < 1 \mu\text{m}$, $\alpha \approx v-2$ (Tomasi *et al.*, 1983). It was assumed that this relationship is valid for all types of aerosols but it is not true (Tomasi *et al.*, 1983 and King and Byrne, 1976). Dubovik *et al.*, (2002) found that the retrieved size distribution of aerosols does not follow Junge power law but they exhibit a bimodal distribution. The departure of this relationship introduces curvature into the $\ln \tau_\lambda$ versus $\ln \lambda$ relationship, it means the logarithm of (1) is not a straight line anymore and the linear fit of $\ln \tau_\lambda$ versus $\ln \lambda$ shows significant deviation from measured AOD whereas the second order polynomial fit to $\ln \tau_\lambda$ versus $\ln \lambda$ is in good agreement with measured AOD (Eck *et al.*, 1999). The second order polynomial equation is given by;

$$\ln \tau_\lambda = a_2 \ln \lambda^2 + a_1 \ln \lambda + a_0 \quad (3)$$

Where a terms are constants and the coefficient a_2 accounts for curvature often observed in Sun photometry measurements. The negative value of curvature indicates that the aerosol-size distribution is dominated by fine mode particles and positive value of curvature indicates the dominance of coarse mode particles (Eck *et al.*, 1999). The second derivative of α is a measure of rate of change of the slope with respect to the wavelength. Using (1) and (3) we have;

Research Article

$$\alpha' = \frac{d\alpha}{d\ln \alpha} = -\frac{d(\ln \tau_\lambda / d\ln \lambda)}{d\ln \lambda} = -2\alpha_2 \quad (4)$$

The second order polynomial fit (Eq. 3) was applied to AOD values at six wavelengths (380, 440, 500, 675, 800, 870 nm). In order to reduce errors especially under low turbidity conditions, only those cases of second order polynomial fit having $R^2 > 0.99$ were considered to minimize the errors (Sharma *et al.*, 2010).

MODIS Aerosol Optical Depth

Satellite data provides information about air quality (Chu *et al.*, 2003 and King *et al.*, 2003). Columnar AOD values derived using MODIS are very useful in order to monitor and study aerosols distribution and their effect over a long time period. MODIS is best suited for such studies because of its revisit cycle of 1-2 days as a result of a close estimate of AOD are made for a given region throughout the year (Prasad *et al.*, 2004). MODIS acquires daily global data in 36 spectral bands from visible to thermal infrared (29 spectral bands with 1-km, 5 spectral bands with 500-m and 2 spectral bands with 250-m, nadir pixel dimensions). The MODIS sensor is onboard the polar orbiting NASA-EOS Terra and Aqua spacecrafts with equator crossing times of 10:30 and 13:30 Local Solar Time, respectively (Levy *et al.*, 2007). Aerosol retrievals over land and ocean surfaces are performed from MODIS data by means of two separate algorithms described in literature with an uncertainty of $\pm 0.03 \pm 5\%$ over ocean and $\pm 0.05 \pm 15\%$ over land (Kaufman and Tanre, 1998; Levy *et al.*, 2010 and Shi *et al.*, 2011). The aerosol properties are derived by the inversion of the MODIS-observed reflectance using pre-computed radiative transfer look-up tables based on aerosol models (Remer *et al.*, 2005 and Levy *et al.*, 2007). The data used in this study include Aqua MODIS aerosol products, calculated using separate algorithms over land and ocean to obtain AOD at 550 nm (AOD₅₅₀). The C005 Level 3 (spatial resolution 1°x1°) MODIS products were obtained from Giovanni website (<http://giovanni.gsfc.nasa.gov/>).

OMI Aerosol Optical Depth

Aerosol Optical depth (AOD) values from the Ozone Monitoring Instrument (OMI) onboard the Finnish-Dutch ozone monitoring instrument that fly on NASA Aura mission, a part of Earth Observation System (EOS) launched in July, 2004. OMI is a nadir viewing spectrometer which measures reflected and backscattered solar light in UV-Visible domain (270-500nm). Although the OMI instrument was primarily designed for trace gases retrieval, it contains valuable information on aerosols. Two separate algorithms have been used for aerosol retrievals from OMI as the OMAERUV and the OMAERO. The OMAERUV algorithm uses only a small range of wavelengths in the near UV from the OMI spectrum, however the OMAERO algorithm uses the wavelength range from 330 to 500nm (Torres *et al.*, 2007). In present case we have used Aura OMI derived Aerosol Data Product-OMAERO (V003) data products obtained from GIOVANNI site (<http://disc.sci.gsfc.nasa.gov/giovanni>).

Black Carbon Mass Concentration

Black carbon (BC) measurements were carried out using seven channels Aethalometer (Model AE-21, Magee Scientific, USA) which provides the real time readout of concentration of black or elemental carbon aerosol particles in an air stream. When the air passes through the quartz fiber filter tape for a fixed amount of time (5 min) with a manually selected constant flow rate (3.5 L m⁻¹ in the present case), aerosols get deposited on the filter tape. The attenuation of light is measured at seven different wavelengths viz. 370, 470, 520, 590, 660, 880, 950 nm when the light beam is transmitted through the aerosols deposited continuously on the fiber filter tape (Hansen *et al.*, 1984). Observations at 880 nm are considered as standard for BC measurement as BC is the principal absorber at this wavelength in comparison to the other aerosol species. The overall uncertainty in BC mass concentration including shadowing effect does not exceed 20% (Babu *et al.*, 2002).

High Volume Sampler

In ambient air dust particles have a size range from a few nanometers to hundreds of micrometer. The mass loading of total suspended particulate matter was measured with the help of high volume air sampler (HVS) that separates the fine and coarse particles viz. RSPM and NRSPM. TSPM was measured by passing air at the flow rate of about 1.03 m³/min through high efficiency cyclone which retains the dust

Research Article

particles greater than 10 micron size and allow only fine (less than 10 micron particles) to reach the glass microfiber filter where these particles are retained. Mass concentration of particles is determined using gravimetric method. In order to avoid clogging of the filter paper, sampling of TSPM was limited to a maximum of twelve hours.

Optical Properties (OPAC)

OPAC (Optical Properties of Aerosols and Clouds) software package is used to estimate the optical properties of composite aerosols over the sampling site, Patiala (Hess et al., 1998) which provide a wide range of possible aerosols compositions and hence is adopted widely (Babu et al., 2002). Depending upon the prevailing atmospheric conditions over the study site a mixture of five types of aerosols as insoluble, water-soluble, BC (soot), mineral (accumulation mode) and mineral transported, are used. Fixing the BC mass mixing ratio (ratio of the mass concentration of BC to the total mass of the composite aerosols), the number densities of other components are varied and a number of iterations are performed so that the estimated AOD and angstrom wavelength exponent are in good agreement with the observed values (Babu et al., 2002). This model permits eight values of relative humidity (0%, 50%, 70%, 80%, 90%, 95%, 98% and 99%) which play an important role for reconstruction of AOD and we used the value closest to the mean relative humidity during the study period. The OPAC-simulated aerosol optical properties are considered satisfactory when the spectral OPAC-AOD is within 5% uncertainty with the measured one via MICROTUPS-II. Various optical parameters such as single scattering albedo (SSA), asymmetry parameter (g) and phase function ($P(\theta)$) of this model are computed using OPAC as a function of wavelength ranging from 0.25 to 4.0 μm .

Aerosol Radiative Forcing (SBDART)

The aerosol radiative forcing is estimated using SBDART code based upon the discrete ordinate radiative transfer. It is used to estimate short-wave clear sky aerosol radiative forcing at surface and top of atmosphere (TOA) in the range of 0.2-4.0 μm . This code is developed by University of California, Santa Barbara for the analysis of radiative transfer problems arising in atmospheric energy budget studies and remote sensing (Ricchiuzzi et al., 1998) and is based upon various physical models which are well tested and reliable. It computes parallel plane radiative transfer in clear and cloudy conditions within the earth's atmosphere and at the surface. The output of OPAC model like single scattering albedo (SSA), aerosol optical depth (AOD), asymmetry parameter (g) and angstrom exponent (α) are used as an input to SBDART to compute aerosol radiative forcing at surface and top of atmosphere (TOA). The albedo is calculated using MODIS albedo product (MODIS/Terra + Aqua albedo 16-day L3 global 1km SIN Grid V005) which provides both white-sky albedo (WSA) as well as black-sky albedo (BSA) for MODIS bands ranging from 0.64-2.13 μm . Using WSA and BSA the actual surface albedo has been calculated. The surface albedo used in the present study is 0.13 ± 0.07 . The direct aerosol radiative forcing involving scattering and absorption of incoming solar radiation by aerosols present in the atmosphere, depends upon nature of aerosols, their size distribution and surface albedo. The detailed explanation about aerosol radiative forcing has been given somewhere else (Sharma et al., 2012). The uncertainties in the short wave ARF calculations could arise due to various factors such as errors in input parameters like AOD, BC mass concentration due to inaccuracy in their measurements and various assumptions involved while using SBDART. The overall uncertainty in ARF calculations does not exceed 20% (Parsad et al., 2007).

RESULTS AND DISCUSSION

MICROTUPS-II based spectral AOD measurements were made on hourly basis on a clear day and then averaged to provide one data set of spectral AOD for that day. Figure 2(a, b) shows the day to day spectral variation of AOD during PoM-2008. Significant day-to-day variations in AOD₅₀₀ values suggested varying aerosol loading over the region during the study period. Figure 2a shows some peaks in AOD₅₀₀ values on certain days and are associated with days of intense paddy residue burning over the region emitting enormous amount of BC in to the atmosphere. A spectral variation of AOD (Figure 2b) reveals that increase in AOD at shorter wavelength is more significant than at longer wavelength

Research Article

attributed to the increased concentration of fine mode particles over the observational site. Spectral AOD remains high from second week of October up to mid of November corresponding to the intense biomass burning activity period and then starts decreasing in the second half of November as the burning activity subsides. The sudden decrease in AOD value to less than 0.6 at 380nm on 16th October can be attributed partly to scavenging of aerosols due to light rain on the previous night and partly to the complete halt of burning activity over the surrounding region as paddy straw became wet due to rain resulting in reduced aerosol loading in to the atmosphere. The monthly mean values of AOD₅₀₀ during October-November, 2008 are 0.92 ± 0.52 and 0.72 ± 0.27 , respectively suggesting high concentration of fine mode aerosols over the region due to biomass burning during this period.

Figure 3(a-b) shows the temporal variation of angstrom exponent α and turbidity parameter β derived from AOD values using least square method (ref). The angstrom exponent α exhibits high values ranging from 0.7 to 1.4 attributed to the abundance of fine mode particles in the atmosphere. There is one to one correspondence between peaks of AOD₅₀₀(Figure 2a) and angstrom exponent α indicating that these days corresponds to excessive loading of BC mass concentration due to intense burning activity around the study region. Turbidity parameter β approaches to a maximum value of 0.77 suggesting that the atmosphere is highly turbid during the study period. Figure 4 shows the scatter plot of coefficient a_2 (measure of curvature of curve between $\ln\tau_\lambda$ versus $\ln\lambda$ as discussed in section 3.1) versus AOD₅₀₀ during the PoM-2008. This curvature of $\ln\tau_\lambda$ versus $\ln\lambda$ depends strongly on the atmospheric conditions prevailing over the measurement site and the angstrom exponent. It is clear in figure that except few cases most of data points are negative and lie away from $a_2 = 0$ line. The negative values of a_2 indicate that the aerosol size distribution is dominated by fine mode particle during PoM-2008 (Eck *et al.*, 1999 and Kaskaoutis *et al.*, 2007). Kaskaoutis *et al.*, (2007) also reported that the departure of $\ln\tau_\lambda$ versus $\ln\lambda$ curve from linearity becomes significant under the conditions of low turbidity and when the fine mode particles are dominant.

In order to quantify the loading of fine mode particles over Patiala during PoM-2008, we have analyzed MODIS derived active fire counts over the region. Figure 5 shows the Aqua-MODIS derived true color composite images on 13th, 27th, 29th October, 2008 and 07th, 12th November, 2008 all over the Punjab region, India. Large number of fire counts and the smoke can be clearly seen from the images over Punjab due to paddy residue burning in the fields during October and November as mentioned in the introduction section. Figure 6(a-c) shows the correlation of ground based MICRTOPS-II derived AOD₅₅₀ with satellite based AOD at 388nm, 442nm and 550nm using Aura-OMI and Aqua-MODIS over Patiala. Figure 6 (a) represents the correlation of AOD₅₅₀ using MICROTOPS-II and Aqua-MODIS exhibiting high correlation coefficient of $R^2 = 0.80$. Similar plots of MICROTOPS-II based AOD with that of Aura-OMI at 388nm and 442nm wavelengths show good correlations with R^2 values of 0.80 and 0.77 respectively (Figure 6b, c) which suggests the possible monitoring of aerosols dynamics over the region using satellite observations with reasonable accuracy.

Particle mass concentration measurements were made with HVS that separates the fine and coarse particles viz. RSPM at PM₁₀ (Respirable Suspended Particulate Matter) and (Non-Respirable Suspended Particulate Matter) NRSPM. Figure 7 shows the day to day variation of RSPM and NRSPM during the whole year of 2008 over the study area. During the PrM-2008 the NRSPM is very high in comparison to RSPM and reaches to a maximum value of $308.2 \mu\text{g}/\text{m}^3$ in the month of May as during this period the atmosphere is highly turbid due to the occurrence of dust storms driven by south-westerly winds. But the opposite result can be seen during the PoM-2008 when the RSPM is high in comparison to NRSPM reaching to a maximum value of $312.6 \mu\text{g}/\text{m}^3$ in the month of November confirming our hypothesis of fine particles emissions due to biomass burning in the fields.

Figure 8 shows the diurnal variation of black carbon aerosol mass concentration during PoM-2008 over Patiala. BC mass concentration shows a maximum in the morning hours (~0900 hours) and minimum in the afternoon hours (1500 hours) during the period of study. The forenoon maximum in BC concentration can be attributed to the shallow atmospheric boundary layer which leads to the accumulation of soot

Research Article

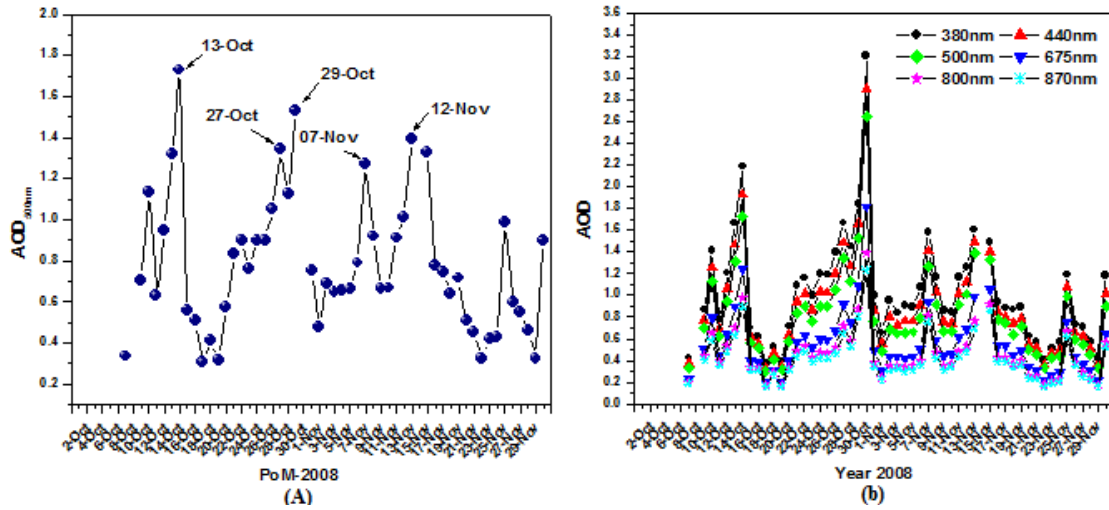


Figure 2: Day to day variation of AOD₅₀₀ and Spectral AOD during PoM-2008

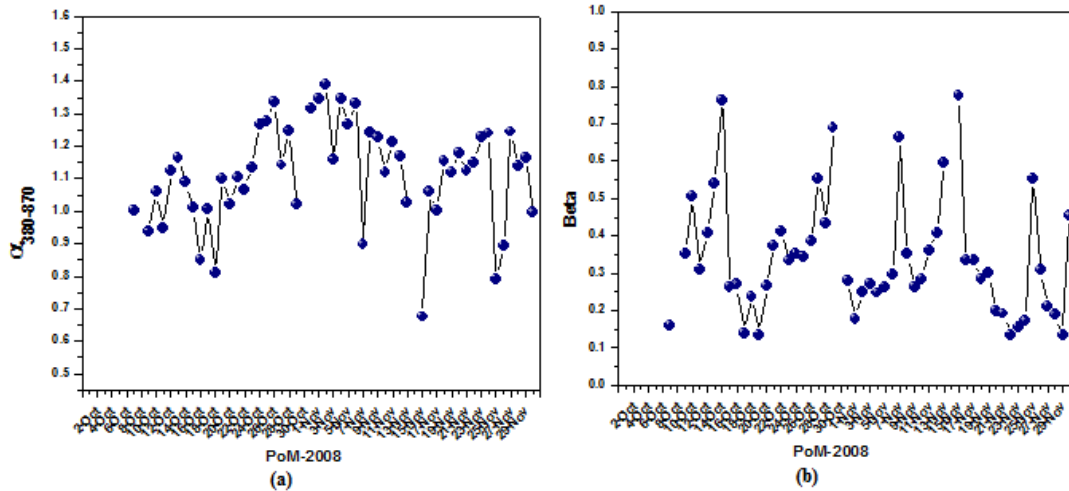


Figure 3: Day to day variation of Ångström coefficients (a) $\alpha_{380-870}$ and (b) β during PoM-2008

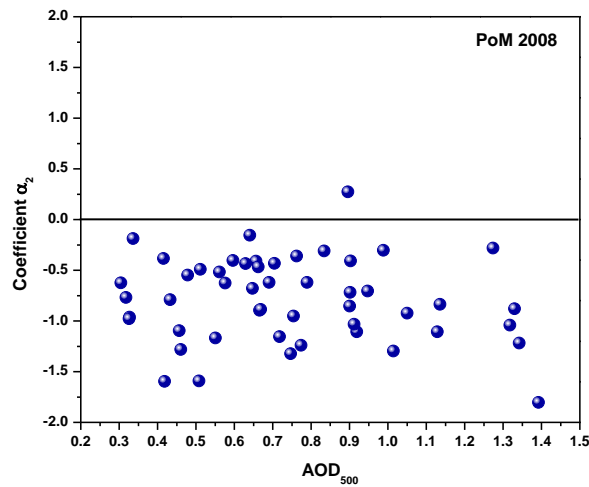


Figure 4: Scatter plot of coefficient a_2 versus AOD₅₀₀ during PoM-2008.

Research Article

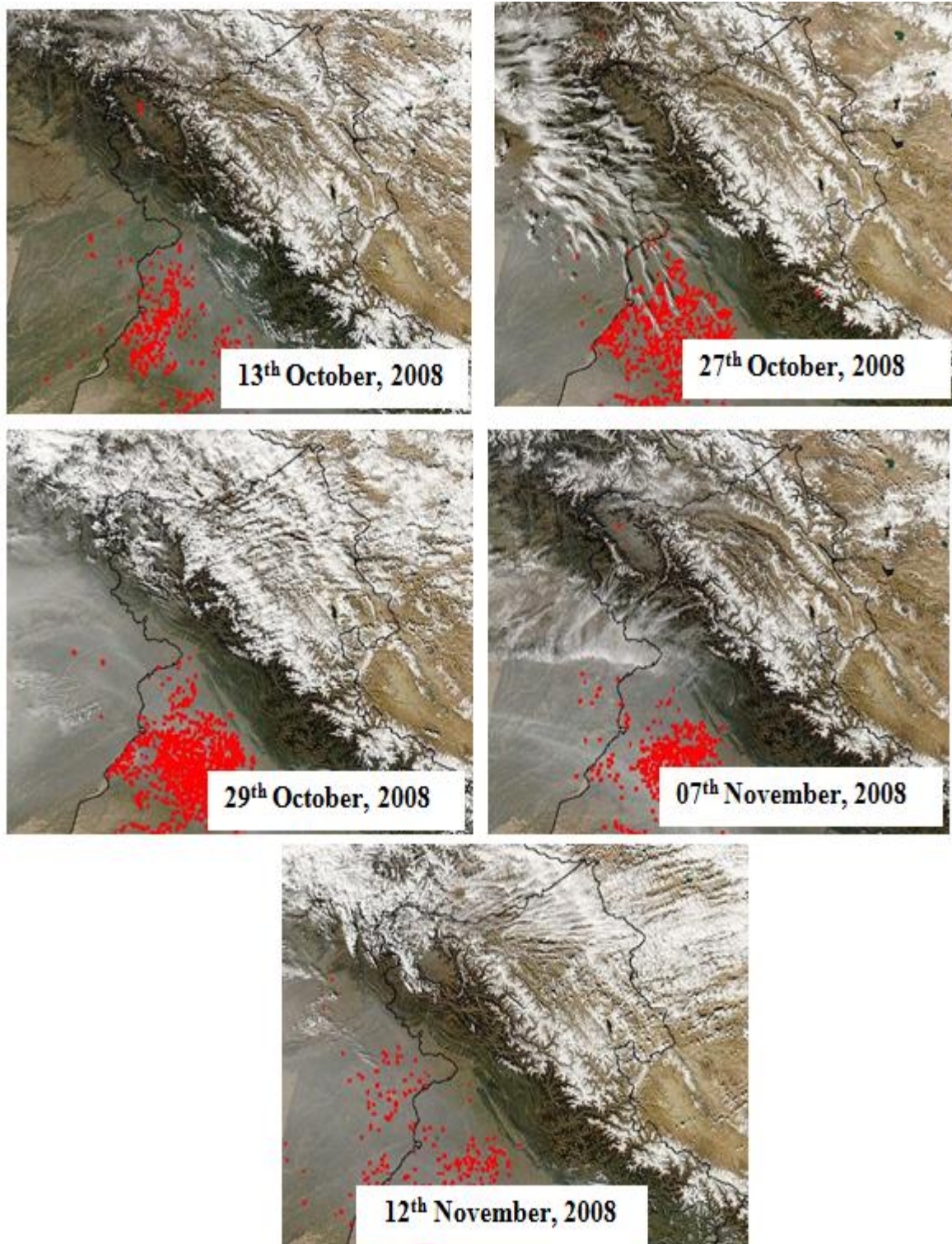


Figure 5: Terra MODIS true color composites showing intense agriculture crop residue burning (red color) and smoke over Punjab state, India during October and November, 2008

Research Article

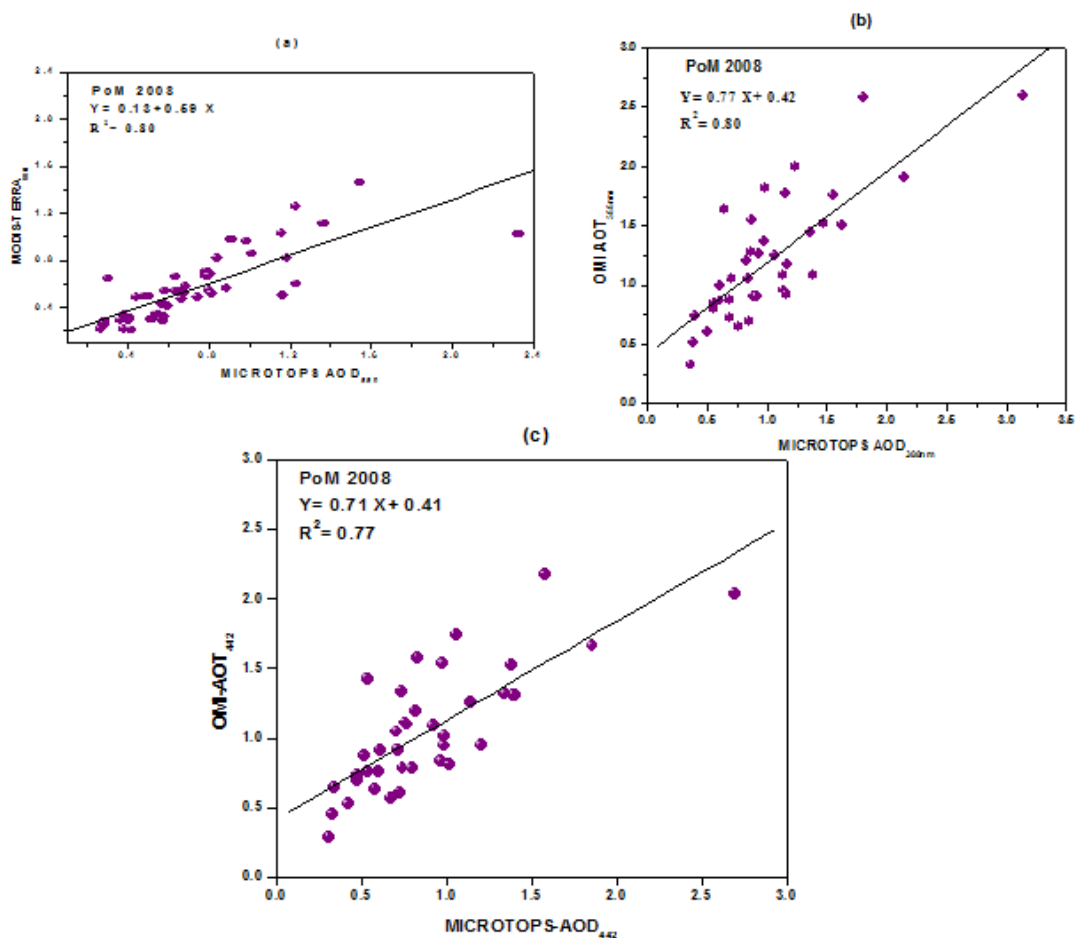


Figure 6: Scatter plot of (a) Terra MODIS AOD₅₅₀ v/s Microtops AOD₅₅₀ (b) OMI AOD₃₈₈ v/s Microtops AOD₃₈₈,(b) OMI AOD₄₄₂ v/s Microtops AOD₄₄₂ over Patiala city, Punjab, India

particles. During afternoon hours, solar heating of Earth’s surface raises the mixing height of the boundary layer. This increase in mixing height of boundary layer lead to the dispersion of aerosols and therefore BC mass concentration attain a minimum during afternoon hours (Badrinath *et al.*, 2009). The daily averaged value of BC concentration ranges between ~7-18 $\mu\text{g}/\text{m}^3$ during the PoM-2008.

SSA plays an important role in determining the effect of aerosols on the planetary system. It is also used as one of the input parameter in radiative transfer codes for the calculation of aerosol radiative forcing. In the present study, the optical properties such as SSA and asymmetry parameter has been obtained using the Optical Properties of Aerosols and Clouds (OPAC) Software package by Hess *et al.*, (1998). Figure 9 shows the spectral variation of SSA for five days corresponding to five intense biomass burning days (13th, 27th, 29th October and 07th, 12th November, 2008). SSA is wavelength dependent and it decreases with increase of wavelength. This decrease in SSA with wavelength is attributed to the presence of abundance of fine mode particles in the atmosphere due to burning practices. The small values of SSA (0.70-0.78) during the intense burning events indicate the presence of abundance of absorbing type aerosols over scattering type aerosols.

Aerosol radiative forcing (ARF) involves scattering and absorption of incoming solar radiation by aerosols present in the atmosphere and at any location it depends upon nature of aerosols, their distribution, SSA, underlying surface albedo and relative humidity etc (Haywood and Boucher, 2000 and Sharma *et al.*, 2012). During present study, the aerosol ARF calculations are computed using the Santa Barbara Discrete-Ordinate Atmospheric Radiative Transfer (SBDART) model developed at university of

Research Article

California, Santa Barbara (Ricchiazzi *et al.*, 1998). ARF calculations were performed in the shortwave range (0.25-4.0 μm) separately at Surface (SRF), top of atmosphere (TOA) and within the atmosphere (ATM). The estimated values of daily averaged SRF, TOA and ATM for five intense burning events (13th, 27th, 29th October and 07th, 12th November, 2008) are shown in Figure 10. The surface radiative forcing is negative in all the cases and varies from -67.1 to -95.0 W m^{-2} . The magnitude of daily averaged TOA forcing is small as compared to surface forcing during the study period and ranges between -3.1 to $+3.7 \text{ W m}^{-2}$. The difference between the TOA and SRF is the atmospheric forcing. The daily averaged atmospheric forcing is positive and varies from $+67.3$ to $+92.7 \text{ W m}^{-2}$ during intense burning events under study.

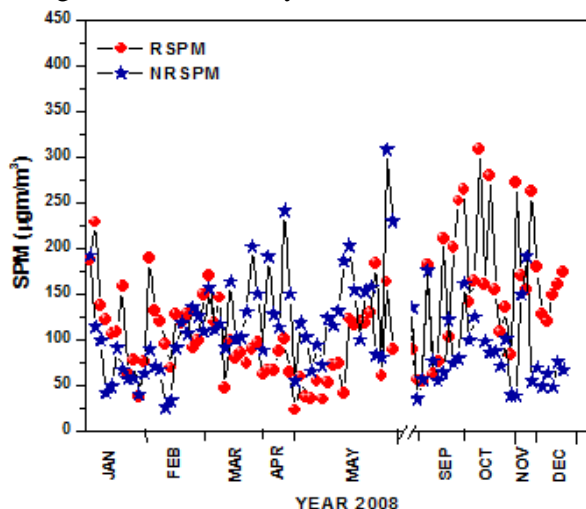


Figure 7: Day to day variation of suspended particulate matter (SPM) during the year 2008.

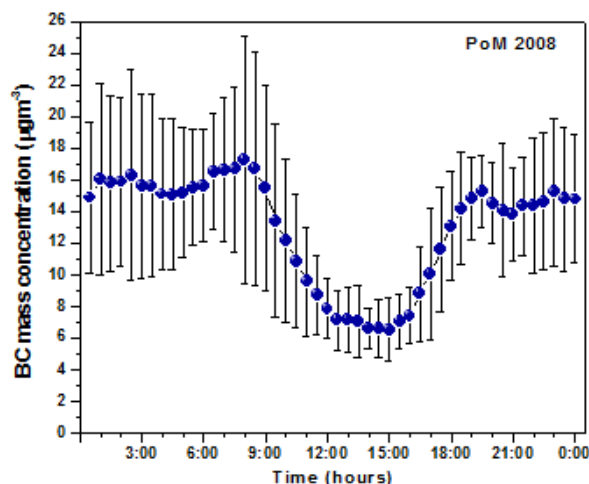


Figure 8: Diurnal variation of black mass concentration (BC) during PoM-2008.

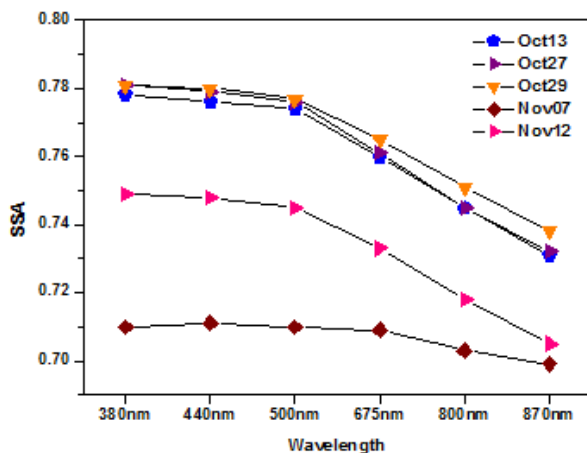


Figure 9: Spectral variation of OPAC-derived SSA values for five intense biomass burning events during PoM-2008.

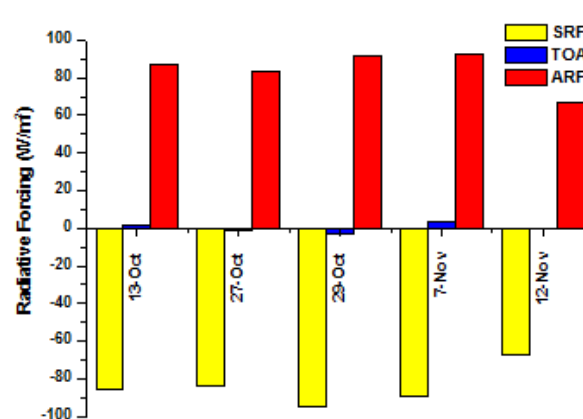


Figure 10: Variation of SRF, TOA and atmosphere (ATM) radiative forcing values for five intense biomass burning events over Patiala during PoM-2008.

Earlier studies by Tripathi *et al.*, (2005) reported a decrease in the shortwave radiation reaching the surface (SRF) $- 62 \pm 32 \text{ W m}^{-2}$ and TOA reflected radiation by $+9 \pm 3 \text{ W m}^{-2}$ during December over Knapur located in the centre of IGP region. Similarly, Badrinath *et al.* (2009) found aerosol forcing of -

Research Article

107.81 W m⁻² at surface over urban region of Hyderabad associated with agriculture crop residue burning. Thus ARF values at the surface and top of the atmosphere at other locations are comparable to ARF over the study region. The high surface cooling (−67.1 to −95.0 W m⁻²) and strong atmospheric heating (+67.3 to +92.7 W m⁻²) over the study region due to agriculture residue burning may affect atmospheric dynamics significantly at the regional level.

ACKNOWLEDGEMENTS

The work is supported under ISRO-GBP research project and the authors are grateful to ISRO for financial support. The authors would like to thank MODIS and OMI science data teams for processing the data via Giovanni website (<http://giovanni.gsfc.nasa.gov/>). We are also thankful to NOAA Air Resources Laboratory (ARL) for the availability of HYSPLIT model online (<http://www.arl.noaa.gov/ready.php>). The meteorological data for Patiala Station provided by IMD is highly acknowledged.

REFERENCES

- Angstrom A (1964)**. The parameters of atmospheric turbidity. *Tellus* **16** 64-75.
- Babu SS, Satheesh SK and Moorthy KK (2002)**. Aerosol radiative forcing due to enhanced black carbon at an urban site in India. *Journal of Geophysical Research Letters* **29** (18) 1880.
- Badarinath KVS, Kiran Chand TR and Prasad VK (2006)**. Agriculture crop residue burning in the Indo-Gangetic plains-A study using IRS P6 AWiFS satellite. *Current Sciences* **91** 1085-1089.
- Badarinath KVS, Sharma AR, Kharol SK and Prasad VK (2009)**. Variations in CO, O₃ and black carbon aerosol mass concentrations associated with planetary boundary layer (PBL) over tropical urban environment in India. *Journal of Atmospheric Chemistry* **62** (1) 73-86.
- Charlson RJ, Schwartz SE, Hales JM, Cess RD, Coakley JA, Hansen JE and Hoffmann DJ (1992)**. Climate forcing by anthropogenic aerosols. *Science* **255** 423-430.
- Chu DA, Kaufman YJ, Zibordi G, Chern JD, Mao J, Li C and Holben BN (2003)**. Global monitoring of air pollution over land from the Earth Observing System- Terra Moderate Resolution Imaging Spectroradiometer (MODIS). *Journal of Geophysical Research* **108**(D21) 4661.
- Dubovik O, Holben BN, Eck TF, Smirnov A, Kaufman YJ, King MD, Tanre D and Slutsker I (2002)**. Variability of absorption and optical properties of key aerosol types observed in worldwide locations. *Journal of Geophysical Research* **105** 9791-9806.
- Eck TF, Holben BN, Reid JS, Dubovic O, Smirnov A, O'Neil NT, Slutsker I and Kinne S (1999)**. Wavelength dependence of the optical depth of biomass burning, urban, and desert dust aerosols. *Journal of Geophysical Research* **104**(31) 349.
- Gautama R, Hsu NC, Tsay SC, Lau KM, Holben B, Bell S, Smirnov A, Li C, Hansell R, Ji Q, Payra S, Aryal D, Kayastha R and Kim KM (2011)**. Accumulation of aerosols over the Indo-Gangetic plains and southern slopes of the Himalayas: distribution, properties and radiative effects during the 2009 pre-monsoon season. *Atmospheric Chemistry and Physics Discussions* **11** 15697-15743.
- Hansen ADA, Rosen H and Novakov T (1984)**. The Aethalometer-An instrument for the real-time measurement of optical absorption by aerosol particles. *Sciences of Total Environment* **36** 191-196.
- Hess M, Koepke P and Schultz I (1998)**. Optical properties of aerosols and clouds: The software package OPAC. *Bulletin of the American Meteorological Society* **79** 831-844.
- Junge CE (1955)**. The size distribution and aging of natural aerosols as determined from electrical and optical measurements in the atmosphere. *Journal of Meteorology* **12** 13-25.
- Jacobson MZ (2001)**. Strong radiative due to the mixing state of black carbon in the atmospheric aerosols. *Nature* **409** 695-697.
- Kharol SK and Badrinath KVS (2006)**. Impact of biomass burning on aerosol properties over tropical urban region of Hyderabad, India. *Journal of Geophysical Research Letters* **33** L20801.
- King MD and Byrne DM (1976)**. A method for inferring total ozone content from spectral variation of total optical depth obtained with a solar radiometer. *Journal of Atmospheric Sciences* **33** 2242-2251.

Research Article

- King MD, Menzel WP, Kaufman YJ, Tanré D, Gao BC, Platnick S, Ackerman SA, Remer LA, Pincus R and Hubanks PA (2003).** Cloud and Aerosol Properties, Precipitable Water and Profiles of Temperature and Humidity from MODIS. *IEEE Transactions on Geosciences and Remote Sensing* **41** 442-458.
- Kaufman YJ and Tanre D (1998).** Algorithm for Remote Sensing of Tropospheric Aerosol from MODIS, Algorithm Theoretical Basis Document, ATBD-MOD-02. *NASA Goddard Space Flight Center* 85.
- Kaskaoutis DG, Kambezidis HD, Hatzianastassiou N, Kosmopoulos PG and Badarinath KVS (2007).** Aerosol climatology: dependence of the Angstrom exponent on wavelength over four AERONET sites. *Atmospheric Chemistry and Physics Discussions* **7** 7347–7397. Available: <http://www.atmos-chem-phys-discuss.net/7/7347/2007/>.
- Levy RC, Remer LA and Dubovik O (2007).** Global aerosol optical properties and application to Moderate Resolution Imaging Spectroradiometer aerosol retrieval over land. *Journal of Geophysical Research* **112** (D13210).
- Lecy RC, Remer LA, Kleidman RG et al., (2010).** Global evaluation of the Collection 5 MODIS dark-target aerosol products over land. *Atmospheric Chemistry and Physics Discussions* **10**(6) 14815-14873.
- Morys M, Mims III FM, Hagerup S, Anderson SE, Baker A, Kia J and Walkup T (2001).** Design calibration and performance of Microtops II handheld ozone monitor and Sun photometer. *Journal of Geophysical Research* **106** 14573-14582.
- Mittal SK, Singh N, Aharwal R. Awasthi A and Gupta PK (2009).** Ambient air quality during wheat and rice crop stubble burning episodes in Patiala. *Atmospheric Environment* **43**(2) 238-244.
- Porter JN, Miller M, Pietras C and Mottel C (2001).** Ship based sun photometer measurements using Microtops Sun Photometers, *Journal of Atmospheric and Oceanic Technology* **18**(5) 765-774.
- Prasad AK, Singh RP and Singh A (2004).** Variability of aerosol optical depth over Indian Subcontinent: Trend and departures in recent years. *Journal of Indian Society of Remote Sensing* **32**(4) 313-316.
- Prasad AK and Singh RP (2007).** Changes in aerosol parameters during major dust storm events (2001–2005) over the Indo-Gangetic basin using AERONET and MODIS data. *Journal of Geophysical Research* **112** ID D09208.
- Ricchiuzzi P, Yang S, Gautier C and Sowle D (1998).** SBDART: A research and teaching software tool for plane-parallel radiative transfer in the Earth's atmosphere. *Bulletin of the American Meteorological Society* **79** 2101-2114.
- Remer LA, Kaufman YJ, Tanre D, Mattoo S, Chu DA, Martins JV, Li RR, Ichoku C, Levy RC, Kleidman RG, Eck TF, Vermote E and Holben BN (2005).** The MODIS Aerosol Algorithm, Products and Validation. *Journal of the Atmospheric Sciences* (62) 947-973.
- Reid JS and Hobbs PV (1998).** Physical and optical properties of young smoke from individual biomass fires in Brazil. *Journal of Geophysical Research* **103**(32) 13-32.
- Sikka DR (1997).** Desert climate and its dynamics. *Current Sciences* **72**(1) 35-46.
- Sharma AR, Kharol SK, Badrinath KVS and Singh D (2010).** Impact of agriculture crop burning on atmospheric aerosol loading—a study over Punjab State, India. *Annales Geophysicae* **28** 367-379.
- Sharma D, Singh D and Kaskaoutis DG (2012).** Impact of two intense dust storms on aerosol characteristics and radiative forcing over Patiala, Northwestern India. *Advances in Meteorology* ID 956814.
- Shi Y, Zhang J, Reid JS, Holben BN, Hyer EJ and Curtis C (2011).** An analysis of the collection 5 MODIS over-ocean aerosol optical depth product for its implication in aerosol assimilation. *Atmospheric Physics and Chemistry* **11**(2) 557-565.
- Tomasi C, Caroli E and Vitale V (1983).** Study of the relationship between Ångström's wavelength exponent and Junge particle size distribution exponent. *Journal of Climate and Applied Meteorology* **22** 1707–1716.
- Torres O, Tanskanen A, Veiheiman B, Ahn C, Braak R, Bhartia PK, Veefkind P and Levelt P (2007).** Aerosols and surface UV products from Ozone Monitoring Instrument observations: an overview. *Journal of Geophysical Research* **112** D24S47.
- Tripathi SN, Dey S, Chandel A, Srivastava S, Singh RP and Holben BN (2005).** Comparison of MODIS and AERONET derived aerosol optical depth over the Ganga Basin, India. *Annales Geophysicae* **23** 1093-1101.